

22 **Abstract**

23 Microplastics are being widely discussed as an emerging global environmental contaminant.
24 Microplastic pollution usually originates from land-based sources, which are then mainly
25 transported through hydrological and atmospheric pathways and accumulated in terrestrial,
26 freshwater and marine ecosystems. Urban environments represent a condensed area of human
27 activities (including the production and use of plastic materials), and urban rivers may therefore
28 be a key transporter of microplastic pollution. Understanding microplastic abundances in urban
29 rivers is potentially important in finding effective means of reducing fluvial microplastic
30 discharge. This study quantified microplastic abundances in surface waters along the Fenghua
31 River, Ningbo, a coastal megacity in East China. Microplastic pollution was distributed
32 unevenly along the river, with concentrations ranging from 300 n/m³ to 4000 n/m³ (0.3 – 4.0
33 n/L). Average concentrations were 1620.16 ± 878.22 n/m³ (1.62 ± 0.88 n/L) in summer (43
34 sampling points) and 1696.08 ± 983.52 n/m³ (1.70 ± 0.98 n/L) in winter (17 sampling points).
35 The most common microplastic shapes, sizes, colors and types of polymers were fiber, <0.5mm,
36 transparent and polypropylene, respectively. Using multidimensional scaling analysis,
37 microplastic distribution patterns were related to seasonal factors and levels of urbanization.
38 No clear relationships were found, with implications for site selection when studying
39 microplastics and the challenges of attributing sources to microplastic pollution in urban rivers.

40 **Keywords:** freshwater, river, microplastics, surface water, urban, China

41

42 **1. Introduction**

43

44 Microplastics refer to plastic debris smaller than 5 mm in diameter. Today, microplastics have
45 been widely documented in global aquatic (Horton et al., 2017), atmospheric (Liu et al., 2020;
46 Zhang et al., 2020) and terrestrial environments (Scheurer and Bigalke, 2018), as well as in
47 biota (Yuan et al., 2019). Ingested and inhaled microplastics may have negative physical and
48 chemical impacts on digestive and respiratory systems associated with abrasion and blockages,
49 as well as leaching toxic monomers and/or additives and other associated pollutants (Di et al.,
50 2019; Rochman et al., 2019; Zou et al., 2017). Microplastics may also accumulate through the
51 food web and could eventually contaminate human food items (Rochman et al., 2019; Zou et
52 al., 2017).

53 The production and consumption of plastic products, as well as mismanaged plastic waste, are
54 the main sources of microplastic pollution (Xu et al., 2020b). By studying these sources,
55 microplastics can be divided into primary (plastic materials produced in micron size, e.g. plastic
56 microbeads) and secondary microplastics (debris physically worn or photodegraded from larger
57 pieces of plastics) (Eerkes-Medrano et al., 2015). Microplastic particles can enter aquatic
58 environments from terrestrial environments via numerous routes including rainfall runoff,
59 sewage discharge, garbage dumping and soil erosion (Horton et al., 2017; Zhang et al., 2018).
60 Fluvial (riverine) environments are usually conduits for the transport of terrestrial microplastics
61 to marine environments (Horton et al., 2017; Pan et al., 2020; Xu et al., 2020b). Globally,
62 marine environments receive and accumulate most of the microplastic pollution discharged
63 from freshwater environments (Caruso, 2019; Eerkes-Medrano et al., 2015; Horton et al., 2017).

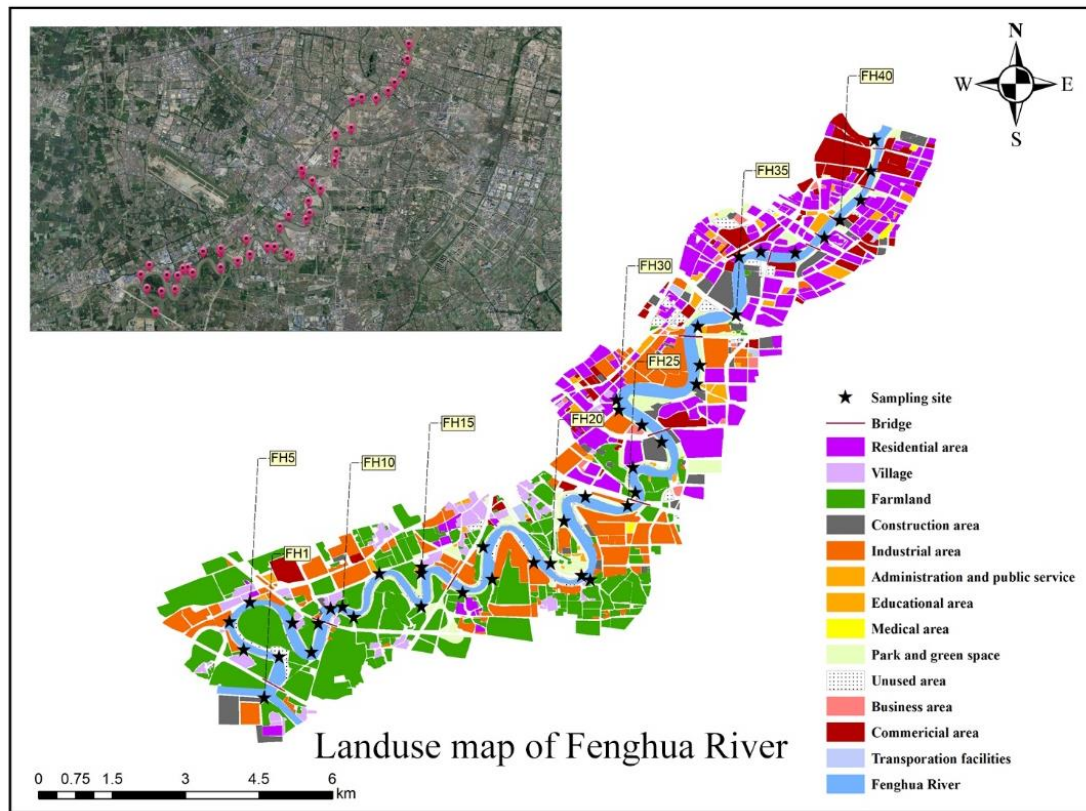
64 China is the largest global producer and consumer of plastic materials (Garside, 2019). The
65 large scale of production and usage of plastic products (including agricultural mulch film,
66 disposable tableware, plastic bags, and synthetic fabrics) has generated large quantities of land-
67 based microplastics (Xu et al., 2020b). So far, the abundance of microplastics has been reported
68 in some major fluvial freshwater environments in China, such as the Yangtze River (Hu et al.,
69 2018; Li et al., 2020; Zhao et al., 2014), Poyang Lake (Liu et al., 2019; Yuan et al., 2019), Taihu
70 Lake (Su et al., 2016), Pearl River (Lam et al., 2020; Ma et al., 2020) and Yellow River (Han
71 et al., 2020), and adjacent oceans of China (Fraser et al., 2020; Wu et al., 2019; Zhao et al.,
72 2014). These show that major Chinese freshwater environments are discharging microplastics
73 into global oceans, with global implications. With China likely to be the leading emitter of
74 microplastics in the world (van Wijnen et al., 2019), paying attention to Chinese freshwater
75 microplastic pollution is important to provide a scientific basis for the discussion of the
76 relationship between microplastic pollution and large-scale human activities.

77 Cities provide multiple sources of microplastics in spatially concentrated areas (Xu et al.,
78 2020a), which are readily transported to other ecosystems, particularly by rivers (Xu et al.,
79 2020b). However, studies on microplastic abundances in urban river catchments remains
80 limited, especially relative to the marine environment (Xu et al., 2020a, 2020b; Zhang et al.,
81 2018), yet critically important in understanding the processes and characteristics of
82 microplastics entering aquatic environments. Thus, this manuscript investigates microplastic
83 pollution in the Fenghua River, which flows through the Chinese coastal megacity Ningbo, in
84 order to quantify concentrations, morphologies and material properties of microplastic
85 pollution, and to relate these variables to surrounding urban land use.

86 **2. Methods**

87 **2.1. Research area and study sites**

88 Ningbo (Fig. 1), Zhejiang Province, is a mega-port city along the eastern coast of China and a
89 new economic center on the southern branch of the Yangtze River Delta (Tang et al., 2015). By
90 2019, the total population of Ningbo exceeded 8.5 million and the Ningbo Port has become the
91 third largest port in the world, in terms of annual container throughput (Lloyd's List, 2019). In
92 the past two decades, rapid urbanization has brought considerable economic development to
93 Ningbo, while at the same time modifying the local land-use planning, economic and
94 population structures (NDRC, 2020). The development of Ningbo City district (population > 4
95 million) has also led to the urbanization of surrounding satellite cities of Ningbo (GOSC, 2020).
96 Among them, the development of Fenghua district (population: 0.2-0.5 million) and Yuyao
97 district (population: 0.5-1 million) is closely related to the major urban rivers of the Ningbo
98 City district (NDRC, 2020; Xu et al., 2020a).



99

100

Fig. 1 Satellite Map of Ningbo Center City and land-use map of Fenghua River

101

102 Ningbo City Center has three major rivers, namely the Yuyao River, Fenghua River and Yong
103 River. The Fenghua River (27-km river length) is an important waterway from south to north,
104 connecting Fenghua City and Ningbo City Center (Fig. 1). It meets the Yuyao River in the
105 middle of Ningbo City Center (Sanjiangkou Estuary), in the commercial center of Ningbo, and
106 then joins into the Yong River downstream. The Yong River flows eastward into Hangzhou Bay,
107 northeast of Ningbo Center City. The upper reaches of Fenghua River are on the outskirts of
108 Ningbo City Center, which are mostly covered by farmlands, villages and industrial areas. The
109 lower reaches of Fenghua River flow through the city center, with high-rise residential buildings,
110 businesses and commercial buildings and other facilities. The variation of the urbanization
111 patterns (from semi-urban to urban) along Fenghua River provides quantifiable variables for
112 investigating the significance of urban factors to microplastic pollution.

113 To consider the influence of urban factors (especially land-use types, population density and
114 GDP) on microplastic concentrations, a spatially dense sampling network was deployed on the
115 urban section of Fenghua River. The sampling was carried out twice; once in July 2019
116 (summer) and once in January 2020 (winter). In July 2019, 43 approximately equidistant
117 sampling points were selected along the river, shown in Figure 2. 31 points were located on the
118 left bank of the river and 12 points were on the right bank because of access limitations. In
119 January 2020, 17 sites were sampled again (Fig. 1), in order to observe the impacts of seasonal
120 factors on urban fluvial microplastic abundance conditions.

121

122 **2.2. Sampling and extracting microplastics**

123 The procedures of microplastic sampling and extracting methods in this research are similar to
124 those in previous research, which have been reviewed by Zhang et al. (2018). The viability of
125 equipment parameters has been verified by Stanton et al. (2020). At each sampling site,
126 stainless-steel buckets were used to collect 30 L of surface water (0-20 cm depth) of the
127 Fenghua River near the bank. The river water was poured from the buckets into a 30L water
128 tank through a stainless-steel sieve (pore size: 0.063 mm) on the bank of the river. This was
129 repeated until the water tank was full. Microplastics suspended or floating in surface water
130 usually have relatively low density and, thus are meaningful in attempting to understand the
131 transportation and of microplastic particles through waterways. The solid residues left on the
132 sieve were washed into a brown glass bottle (250 ml) using deionized water, representing a
133 sample of particulate matter at that site. The glass bottle was sealed by aluminized paper to
134 avoid contamination and then brought back to the laboratory for microplastic extraction. If
135 necessary, the samples were preserved for a short time (< 14 days) under the conditions of low
136 temperature and avoiding light inputs.

137 In the laboratory, 30% hydrogen peroxide (H₂O₂) solution was mixed with the water sample in
138 a larger transparent glass bottle (500ml). The mixed solution was heated in a water bath for 5
139 hours at a temperature of 80°C. The purpose of this step is to digest the bio-organic matter in
140 the sample. Subsequent to the solution cooling, the sample was filtered again with a stainless-
141 steel sieve (pore size: 0.063 mm). The solid residue left on the screen was washed into a
142 centrifugal tube by saturated sodium chloride solution (1.2 g/ml). Then the centrifugal tube was
143 centrifuged at a speed of 4000 rpm for 5 minutes to separate impurities (e.g., sediments) from
144 microplastics through density differences. With the help of a vacuum pump, the upper layer of

145 centrifuged liquid, was filtered through a nitrate cellulose membrane with a pore diameter of
146 0.45 μ m (114H6-47-ACN, Sartorius, Germany). The residues on the filter membrane were
147 suspected to be microplastics. The filter membrane containing suspected microplastics was
148 stored in a covered glass dish, protected from light, for later observation and identification.

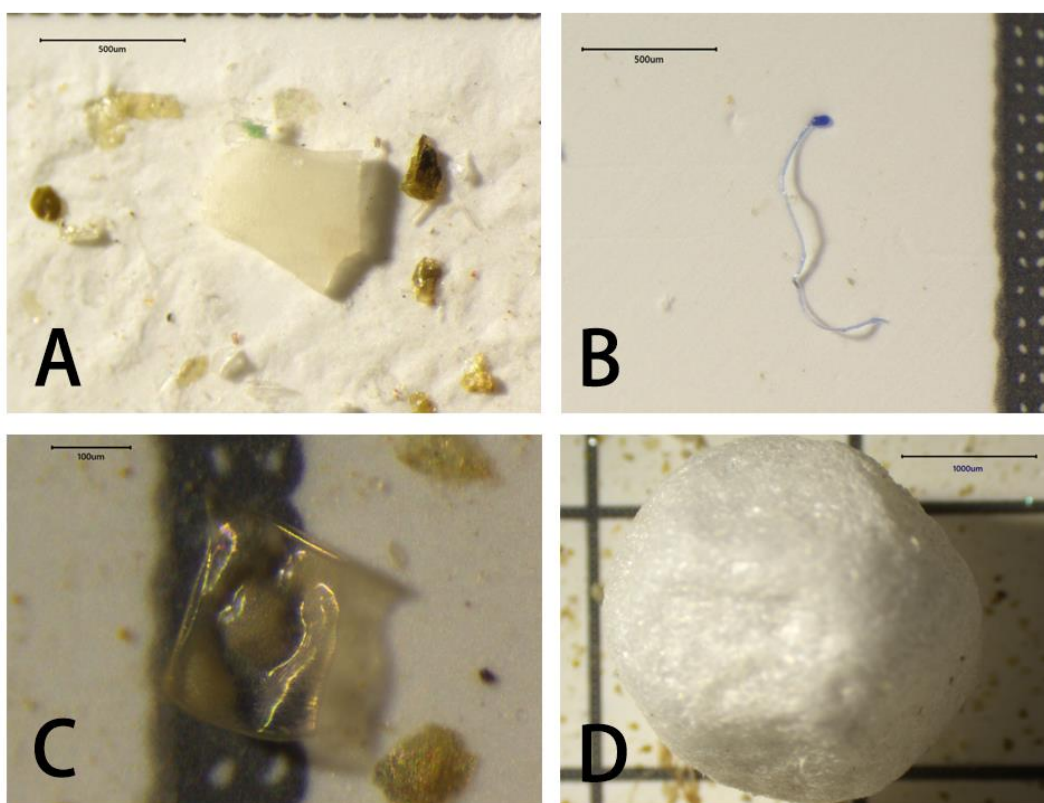
149

150 **2.3. Identification of microplastics**

151 A stereomicroscope (S9D 170x, Leica, Germany) equipped with a digital camera (MD170,
152 Leica, Germany) was used to visually identify suspected microplastics on each filter membrane,
153 to distinguish obvious impurities (such as minerals, diatom skeletons and freshwater sponge
154 spicules). Meanwhile, the size, color, shape and number of suspected microplastics were
155 recorded.

156 Confirmation of suspected microplastics, as well as their polymer composition was identified,
157 using *Fourier Transform Infrared Spectrometer* (FTIR) (Vertex 70, Bruker, Germany) equipped
158 with *Attenuated Total Reflection* (ATR) accessory (A225/Q Platinum ATR Diamond F. Vacuum,
159 Bruker, Germany). *OPUS 7.0.129 software* (Bruker, Germany) installed with *BrukerOptics SH*
160 *spectrum* libraries were used to compare the detected and standard spectrums for polymers.
161 Due to the limitations of the technique, suspected microplastics with sizes less than 0.5 mm
162 were too small to be identified using ATR-FTIR. Therefore, the evaluation of the accuracy of
163 microplastic identification could only be achieved on larger particles, a limitation shared with
164 other studies that used a similar approach (e.g. Stanton et al., 2019; Zhao et al., 2020).

165 In this study, microplastics were divided into four shapes: fragment, fiber, film and pellet/foam
166 (Fig. 2). It is difficult to identify fibrous microplastics using ATR-FTIR because of their small
167 diameters. Whilst confidence in the visual identification of fibers was increased through the use
168 of FZT01057.3-2007 national standard document of China for identifying natural and synthetic
169 fibers (NDRC, 2007), their polymer composition could not be identified. As a result, the
170 polymer type of fibrous microplastics were not recorded in this study.



171

172 *Figure 2 Hard plastic debris with irregular shapes (A), linear or wire-like synthetic materials*
173 *(B), soft and flat plastic debris (C) and spherical or nearly spherical plastic materials (D)*
174 *observed in this study were classified as microplastic fragments, fibers, films and*
175 *pellets/foams*

176

177 **2.4. Quality assurance and quality control (QA/QC)**

178 In this study, a total of 77 suspected microplastics were identified by ATR-FTIR. 65 of those
179 were identified as artificial polymers while another 12 pieces as natural or non-polymer
180 materials. Therefore, the recognition accuracy of microplastics by microscopic identification
181 could be up to 84.4%. However, considering that most of the suspected microplastics with
182 smaller sizes and those with fibrous morphology were only identified with microscopy, it is
183 possible errors in identification are large. Potential overestimation or underestimation of the
184 results will be discussed in following sections.

185 To avoid contamination, non-plastic sampling tools and sample storage items were preferred.
186 For tools that were made of plastic, products with obvious colors and high material density
187 were selected because plastics with density higher than 1.2g/cm^3 were excluded during the
188 process of centrifugal flotation and plastic debris from contamination could be distinguished
189 according to its color. For example, orange plastic spray cans were used to carry deionized
190 water during fieldwork, and no orange microplastics were found in samples.

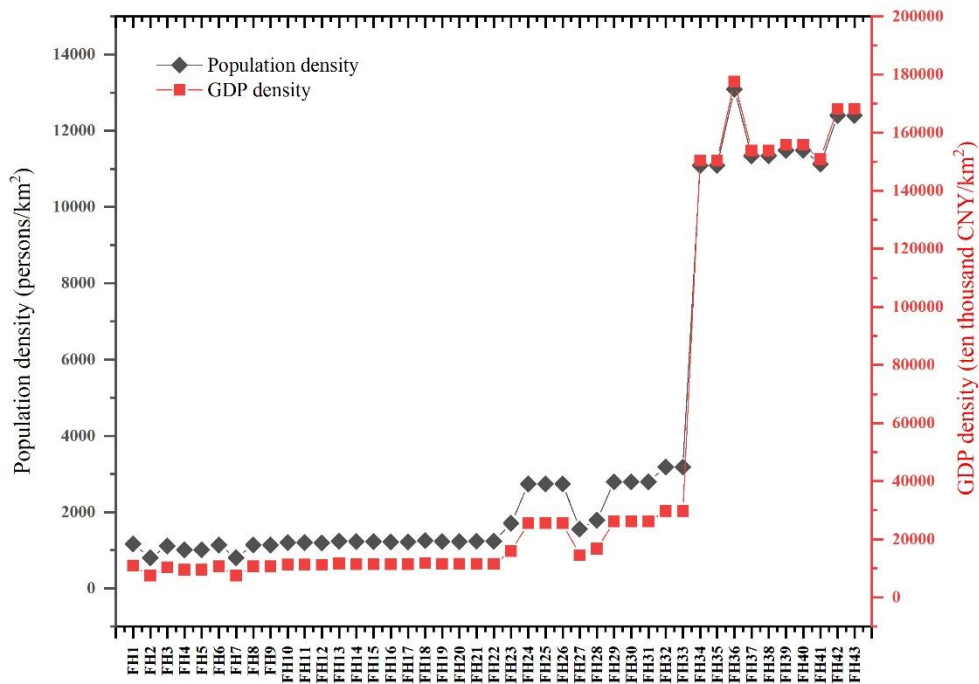
191 In the laboratory environment, samples were sealed or protected by aluminum foil or a glass
192 cover when stored. During the microscopic examination of suspected microplastics, non-plastic
193 particles in small size ($<1\text{mm}$) were also excluded by observing whether cellulose texture or
194 cell veins exist on the particle surface and whether the particle is easily broken under slight
195 pressure by a metal tweeze or dissecting needle. Meanwhile, three blank samples with
196 deionized water went through the same pretreatment and laboratory work process before
197 observation, to evaluate background contamination levels.

198

199 **2.5. Statistical approaches**

200 From past studies of urban microplastic abundance patterns, (a) the distance from sampling
201 sites to city center, (b) land-use types, (c) population density and (d) local economic structure
202 (usually with gross domestic product (GDP) as an index) have been considered as potential
203 factors (Fan et al., 2019; Peng et al., 2018; Wang et al., 2017). This paper employed linear
204 regression and Kruskal-Wallis tests to analyze the above four factors, statistically. The order of
205 sampling points from upstream to downstream and the straight-line distance from sampling
206 points to city center were both considered in the distance analysis. A map of the land-use
207 conditions within 1 km of each bank was drawn according to a combination of the “*Essential*
208 *Urban Land Use Categories*” map of Ningbo (Gong et al., 2020), records taken during
209 fieldwork, and satellite images. According to this map (Fig. 1), we classified the land-use type
210 of each sampling site (see sampling site geographic information in Tab. S1). A raster map with
211 the population density and GDP density data (for 2015) were used to determine the population
212 and GDP size of each site (Geographical Information Monitoring Cloud Platform, 2020a,
213 2020b).

214 It is worth noting that the unit population density and unit GDP density of 43 sampling sites
215 have similar trends (Fig. 3). According to this pattern, we classified FH1-FH22 into semi-urban
216 areas, FH23-FH33 as transition area and FH34-FH43 as urban center area and applied Kruskal-
217 Wallis analysis to evaluate the differences of microplastic concentrations with varying
218 urbanization level.



219

220 *Figure 3 Population density (Black) and GDP density (Red) of 43 sampling sites*

221

222 In Ningbo, the urban inland river network covers sub-catchments of different city blocks and
 223 flows into the urban mainstream through sluice gates. 18 of 43 sampling points were adjacent
 224 to those sluices in this study. Those sluices could be point sources of microplastic pollution
 225 along Fenghua River because they regulate the water level and flow. A Mann-Whitney U test
 226 was used to evaluate whether the sluices contribute to microplastic discharge events. In addition,
 227 a Wilcoxon test was used to detect the seasonal difference in microplastic pollution in the
 228 Fenghua River. All statistical works were conducted in *IBM SPSS Statistics 23*.

229 Because microplastics concentrations and morphologies may not vary in response to any single

230 dominant variable, this study also utilized non-metric multidimensional scaling analysis
231 (NMDS) to assess the Bray-Curtis dissimilarities of microplastic concentrations and typology
232 between sampling sites at the same time, which was completed under the environment of
233 *RStudio 1.4*.

234

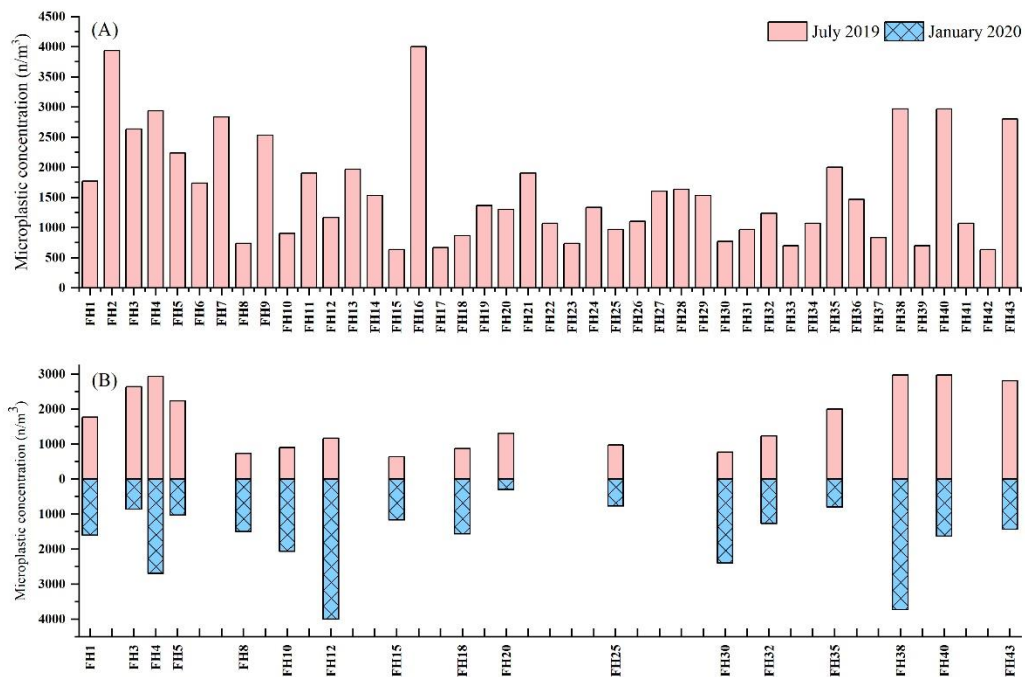
235 3. Results

236 3.1. Microplastic concentration

237 Microplastics were detected in all 43 summer samples (July 2019) and 17 winter samples (Jan
238 2020) (Fig. 3). The average microplastic concentration in the 43 summer samples was 1620.16
239 ± 878.22 n/m³, the maximum value was 4000.00 n/m³ at site FH16, and the minimum value
240 was 633.33 n/m³ at FH15 and FH42. The 17 sites sampled in winter had an average microplastic
241 concentration of 1696.08 ± 983.52 n/m³, the maximum value was 4000.00 n/m³ at FH12, and
242 the minimum value was 300.00 n/m³ at FH20. The equivalent summer values for the same 17
243 sites were : average 1698.04 ± 863.23 n/m³ , maximum 2966.67 n/m³ at FH40, and minimum
244 633.33 n/m³ (FH15) (Fig. 4 & 5). There were two outliers during summer, which had very high
245 concentrations; FH2 (3933.33 n/m³) and FH16 (4000.00 n/m³) (Fig. 4 & 5). In winter, there
246 were also 2 outliers, with similarly high concentrations but at different sites; FH12 (4000.00
247 n/m³) and FH38 (3733.33 n/m³) (Fig. 4 & 5).

248 The concentrations of microplastics detected in the three blank samples were 100.00 n/m³,
249 100.00 n/m³ and 166.67 n/m³, respectively. This is likely derived from airborne contamination

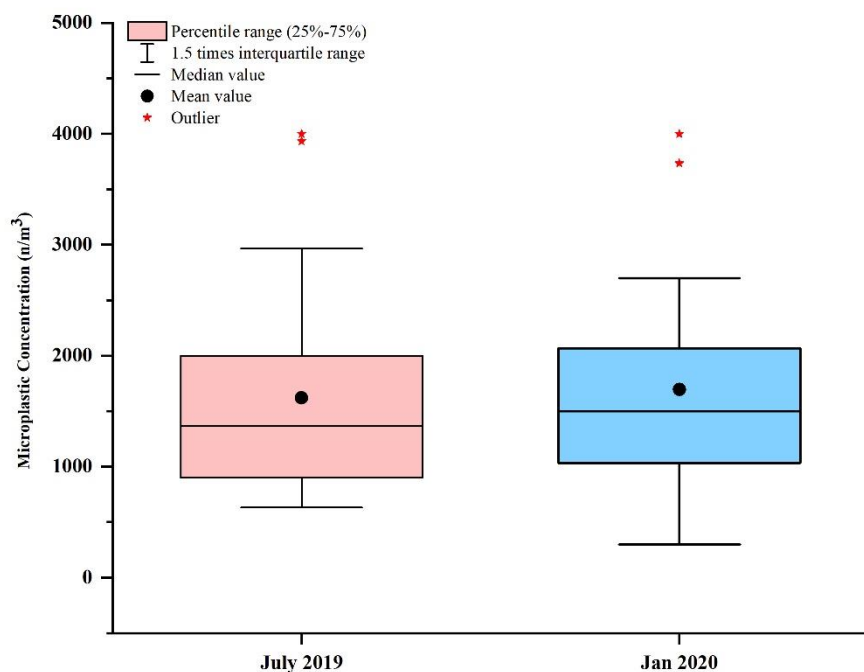
250 in periods of collection and identification between samples between covered. As these values
 251 were consistent and small relative to mean and minimum values, they were not used to correct
 252 sample concentrations.



253

254 *Fig. 4 Microplastic concentrations at 43 summer sampling sites (A) and the 17 sampling sites*

255 *investigated during both July 2019 (B, red) and January 2020 sampling sites (B, blue)*



256

257 *Fig. 5 Quartile box chart of 43 summer (red) and 17 winter samples (blue) of Fenghua River,*

258

Ningbo

259

260 **3.2. Microplastic properties**

261 Among the four recorded shapes of microplastics, fiber was, on average, the most common

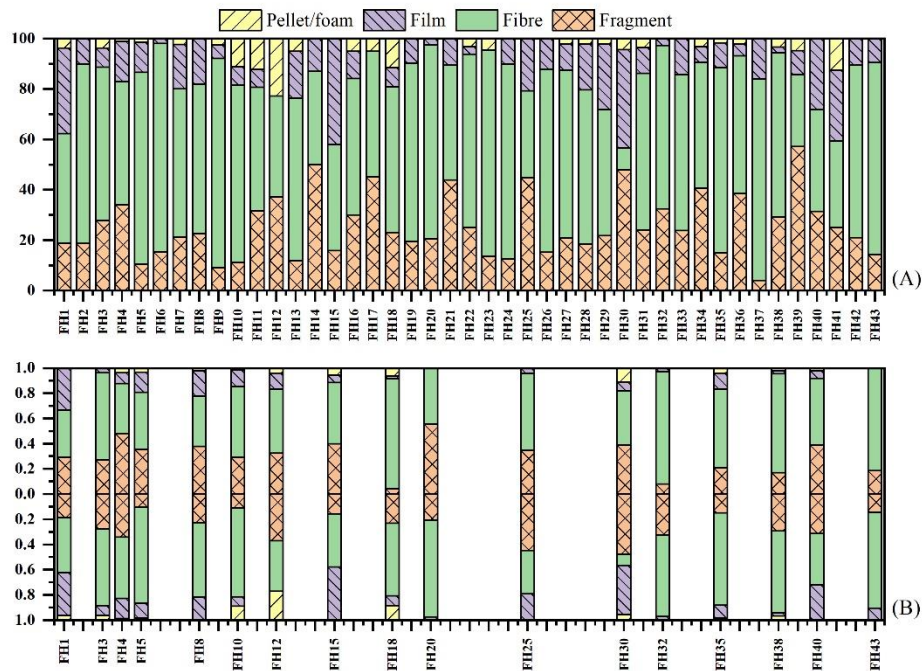
262 across the summer and winter samples (Fig. 6). Of the 43 summer samples, the percentage of

263 fibers ranged from 9-83%; fragments ranged from 4-57%; films were 0-42%; and pellet/foam

264 ranged from 0-23% of the total particles. Among the 17 winter samples, the range in the

265 percentage of total for fibers, fragments, films and pellets/foams were 38-89%, 4-56%, 0-33%

266 and 0-11%, respectively.



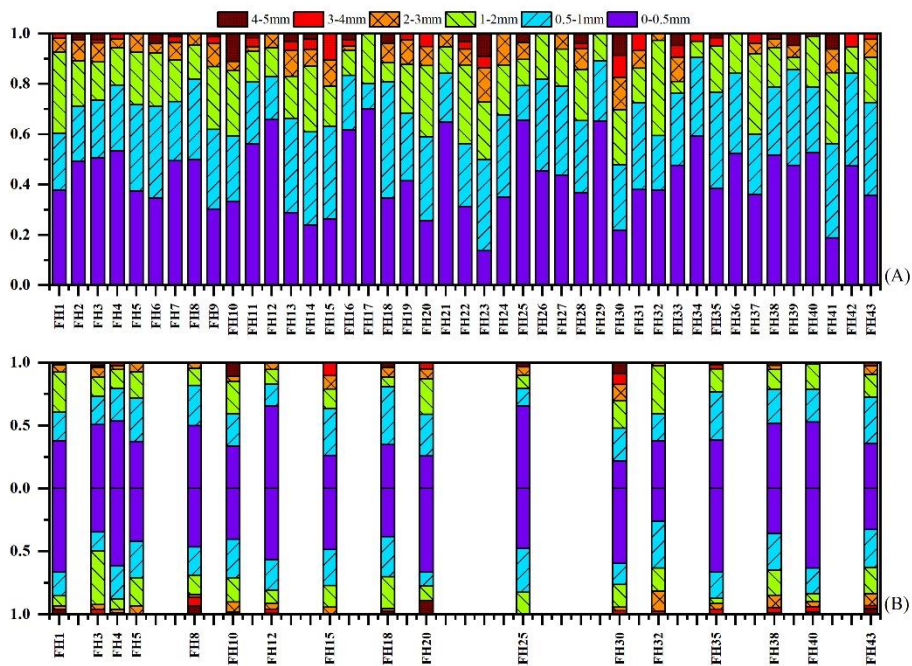
267

268 *Figure 6 The proportion of four microplastic shapes between 43 sampling sites during*
 269 *summer (July 2019) (A) and 17 sampling sites during summer (B, above zero scale) and*
 270 *winter (January 2020) (B, below zero scale).*

271

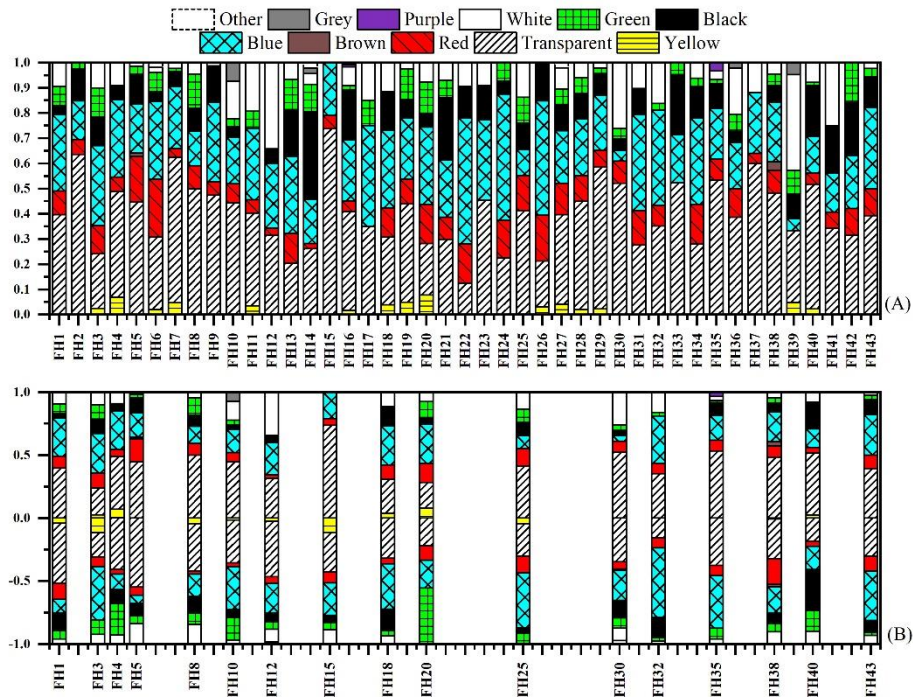
272 According to size, microplastics were divided into six groups (0 – 0.5mm, 0.5 – 1mm, 1 – 2
 273 mm, 2 – 3 mm, 3 – 4 mm, 4 – 5 mm). Microplastics with diameters smaller than 0.5 mm were
 274 the most common in samples, accounting for 14-70% of 43 summer samples and 26-67% of 17
 275 winter samples, with an average of $72.19 \pm 10.88\%$ below 1 mm ($74.19 \pm 10.30\%$ for winter)
 276 (Fig. 7). More than 10 colors of microplastics were observed. Transparent microplastics were
 277 the dominant type, accounting for 13-74% during summer and 16-55% in 17 winter samples
 278 (Fig. 8). In addition, blue, black and white were also observed frequently.

279 Three major types of polymers were identified using ATR-FTIR; polypropylene (PP, 57%),
 280 polyethylene (PE, 35%) and copolymer (8%). Detected PP and PE also contained different
 281 types of materials, such as polypropylene with different molecular weights, Low Density
 282 Polyethylene (LDPE) and ultra-high-molecular-weight polyethylene. The compositions of the
 283 copolymers were also diverse, including PE-Ceresin copolymer, PP-PE-acrylonitrile-styrene
 284 copolymer and styrene-allyl alcohol copolymer. This means although the types of polymers
 285 were similar, the uses of them are likely to be varied.



286

287 *Figure 7 The proportion of microplastic size groups between 43 sampling sites during*
 288 *summer (July 2019) (A) and between 17 sampling sites in summer (B, above zero scale) and*
 289 *winter (January 2020) (B, below zero scale).*



290

291 *Figure 8 The proportion of microplastic colors between 43 sampling sites during summer*

292 *(July 2019) (A) and between 17 sampling sites in summer (B, above zero scale) and winter*

293 *(January 2020) (B, below zero scale).*

294

295 3.3. Statistical analysis results

296 There was no significant linear correlation between microplastic concentration and the straight-

297 line distance from sampling sites to the city center (R^2 of 43 summer samples = 0.054; R^2 of 17

298 winter samples = 0.103). The order of 43 sampling points (from upstream to downstream) had

299 no linear relationship with microplastic abundance conditions (see detailed R^2 values in Tab. S2).

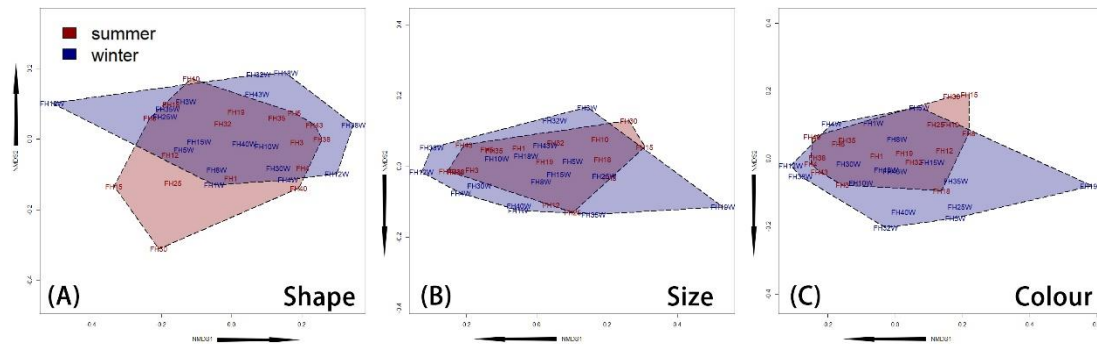
300 There was also no significant relationship between microplastic concentration and the

301 population density, or between microplastic concentration and GDP density (Tab. S2). Kruskal-

302 Wallis tests failed to find significant statistical differences of microplastic concentration among
303 different land-use types (total microplastic concentration, $p = 0.717$) and different urbanisation
304 levels (total microplastic concentration, $p = 0.171$) (Tab. S3&S4).

305 Mann-Whitney tests similarly did not distinguish significant differences between total
306 microplastic concentrations at 18 sampling sites with water sluices and the 25 sampling points
307 without sluices ($p = 0.325$, Tab. S5). However, the concentrations of microplastic films were
308 found have significant differences between sites with and without sluices ($p = 0.048$, Tab. S5).
309 Microplastic concentrations of the 17 winter and summer samples were statistically similar
310 (Wilcoxon test; $p = 0.723$, Tab. S6).

311 Non-metric multidimensional scaling results of microplastic concentrations in different
312 categories are shown in Fig. 9 & S1. Stress values of n-MDS graphs are between 0.039 and
313 0.140, which represents high scaling quality. In the same coordinate system, as the distance
314 between two points decreases, the similarity between them increases. In Fig. 9 & S1, X-axis
315 (NMDS1) indicates a changing trend of microplastic concentration (black arrow shows positive
316 direction) whereas the evenness of microplastic types vertically changed (black arrow shows
317 positive direction) along Y-axis (NMDS2) (i.e. sites dominated by a single type of microplastic
318 have low evenness). The results of the NMDS indicate no clear relationships or explanatory
319 drivers of the between-site pattern in microplastic presence, supporting earlier, linear analysis.



320

321 *Figure 9 NMDS coordinate graphs of 17 repeated sampled sites for microplastics in four*
 322 *shapes (A) (Stress = 0.106), six size ranges (B) (Stress = 0.081) and eleven colors (C) (Stress*
 323 *= 0.120). Horizontal axis of each graph is the first non-metric dimension scale (NMDS1), and*
 324 *the vertical axis is the second non-metric dimension scale (NMDS2). Summer points are in*
 325 *red and winter points are in navy. Hull polygons seal the points of different seasons.*

326

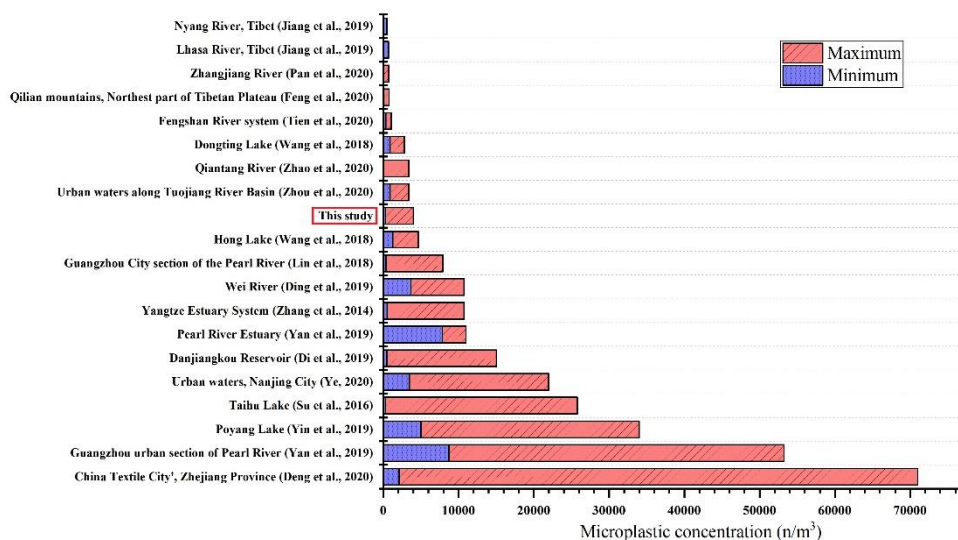
327 4. Discussion

328 4.1. Overall microplastic pollution condition

329 4.1.1. Microplastic concentration level

330 The microplastic concentration range in the Fenghua River was 300-4000 n/m³ (refer Fig. 4 &
 331 5). When compared to the 19 previous studies on microplastic pollution in Chinese freshwater
 332 environments, the microplastic concentrations in the Fenghua River are relatively mild and
 333 similar to concentrations recorded in the urban sections of Tuojiang River, Qiantang River,
 334 Dongting Lake and Hong Lake (Wang et al., 2018; Zhao et al., 2020; Zhou et al., 2020) (Fig.
 335 10). The Qiantang River flows through Hangzhou City, Zhejiang, which is the neighboring

336 catchment to Ningbo with broadly similar geographical conditions. It is therefore noteworthy
 337 that the characteristics of microplastic pollution (including shape, size and color distributions)
 338 in the Qiantang River were similar to those in Fenghua River (Xu et al., 2020a; Zhao et al.,
 339 2020). Microplastic concentrations were lower in the Fenghua River than those recorded in the
 340 Pearl River Basin and Yangtze River Estuary (Fig.10). This may be because the population size
 341 in Ningbo (> 8 million) is relatively small compared to the cities in Pearl River Basin (e.g.
 342 Guangzhou: > 15 million; Shenzhen > 13 million) and in the Yangtze River Basin (e.g.
 343 Shanghai: >24 million) (National Bureau of Statistics of China, 2020). The microplastic
 344 concentration in the Fenghua River is also lower than that recorded in Taihu Lake, Poyang Lake
 345 and other large lakes (Su et al., 2016; Yuan et al., 2019) (Fig. 10). This is likely because lakes
 346 act as sinks, accumulating microplastic through time.



347
 348 *Figure 10 Microplastic concentration ranges of this study and previous publications about*
 349 *microplastic pollution in surface water of Chinese freshwater environments (Deng et al.,*
 350 *2020; Di et al., 2019; Ding et al., 2019; Feng et al., 2020; Jiang et al., 2019; Lin et al., 2018;*

351 *Pan et al., 2020; Su et al., 2016; Tien et al., 2020; Wang et al., 2018; Yan et al., 2019, 2019;*
352 *Ye, 2020; Yuan et al., 2019; Zhao et al., 2014, 2020; Zhou et al., 2020)*

353

354 **4.1.2. Microplastic characteristics**

355 Fibers were the most common microplastic shape along the Fenghua River, which is consistent
356 with the results of previous research in China (Fig. 6) (Lin et al., 2018; Xu et al., 2020b; Yan et
357 al., 2019), indicative of domestic sewage, waste fabrics, and fishery activities (Xu et al., 2019;
358 Xue et al., 2020). Numerous clothing/garment factories in Ningbo may be an important source
359 of detected microplastic fiber pollution (Tang et al., 2015; Xu et al., 2020a). It is also worth
360 noting that during the visual identification of microplastics in this study, the amounts of natural
361 fibers (including cotton and wool) was much higher than that of synthetic fibers, supporting
362 recent recognition of the prevalence of these non-plastic anthropogenic particles in freshwater
363 (Stanton et al., 2019), marine (Suaria et al., 2020) and biota (Guen et al., 2019) microplastic
364 surveys. The widespread abundance of natural fibers may impact the accuracy of microplastic
365 fiber identification in this, and other, studies.

366 In terms of size, most of microplastics detected in the Fenghua River were smaller than 1 mm
367 (Fig. 6). This result is consistent with previous studies on freshwater basins in China (Xu et al.,
368 2020b; Zhang et al., 2018; Zhao et al., 2020), although direct comparison of size ranges is
369 challenging because different studies have used different mesh sizes when extracting plastics.
370 Microplastics of smaller size will have higher bioavailability, which may increase ecological
371 risks (Zou et al., 2017). It takes time for macro-plastics to breakdown into smaller plastic

372 particles through physical wear or degradation in the environment (Horton et al., 2017;
373 Lehtiniemi et al., 2018). Therefore, the abundance of smaller microplastics (<1 mm) in Fenghua
374 River may indicate that plastic pollution in Chinese freshwater environments has a relatively
375 long history. Further observations and research is required on the implications of the
376 microplastic size range in Chinese freshwater environments on potential ecological risks (Dong
377 et al., 2020).

378 Transparent microplastics were observed most frequently along the Fenghua River, which is
379 similar to previous studies (Fig. 7) (e.g. Zhang et al., 2018; Zhao et al., 2020). Some studies
380 used color as an indicator of possible sources (Ding et al., 2019; Eerkes-Medrano et al., 2015).
381 For example, transparent film microplastics may come from agricultural mulch of plastic bags,
382 while brightly colored microplastic fragments may come from the decomposition of plastic
383 industrial products (Jiang et al., 2019; Tien et al., 2020). The digestion of organic matter with
384 hydrogen peroxide solution may also digest some dye additives in plastic materials, resulting
385 in the potential discoloration of microplastics (Crawford and Quinn, 2017). In this research, a
386 number of microplastics showed signs of discoloration, such as fibers faded from blue to
387 transparent and fragments from green to light blue. Therefore, we do not recommend using
388 microplastic colors as a basis for speculating microplastic sources. Nonetheless, the diversity
389 of colors found in this study is likely to imply a diversity of pollution sources.

390 PP and PE were the most common polymer types in the surface water along the Fenghua River,
391 consistent with other publications of microplastics in Chinese freshwaters (Li et al., 2019; Xu
392 et al., 2020b; Zhang et al., 2018). PP and PE are the two most widely used artificial polymer

393 materials in China, involved in plastic packaging and agricultural mulch (Lam et al., 2020).
394 Most of the co-polymers found along the Fenghua River were plastic foam materials, most
395 likely derived from plastic packaging associated with e-commerce and express delivery
396 services (Industry, 2019). As a coastal megacity with rapid economic development, Ningbo has
397 seen rapid increases in the fields of e-commerce and express business (Li and Yang, 2016). This
398 may explain the dominant distribution of PP and PE in surface water. Compared to other studies,
399 fewer polymers types were detected in Fenghua River, for example, polyethylene terephthalate
400 (PET) has been commonly found in surface waters in other Chinese studies (e.g. Zhang et al.,
401 2018). The dominance of PP and PE in our surface water samples is also likely to partially relate
402 to them having lower density than some other plastic materials, which would be more likely to
403 sink and be present deeper in the water column or in the sediments.

404

405 **4.2. Microplastic distribution pattern**

406 **4.2.1. Seasonal variation**

407 First, although there were differences between the sampling points in terms of microplastic
408 concentration, shape, size, color and polymer type, the variations between seasons were not
409 significant according to Wilcoxon tests (Tab. S6). Nonetheless, according to n-MDS analysis,
410 it is possible to tentatively describe some patterns (Fig. 9). On the aspect of shape, size and
411 color, winter polygons in Fig. 9 (A, B & C) have a larger range along the horizontal axis, which
412 means a larger distribution range of winter points in terms of microplastic concentration.

413 Similarly, winter samples have a larger variation in the size and color of microplastics (Fig. 9
414 B & C). If the summer outlier FH30 is removed, the vertical distance of the summer polygon
415 is also smaller than that of winter polygon (Fig. 9A). These features indicate that microplastic
416 concentrations and types between the 17 sampling sites were more similar in summer than in
417 winter. July and January are respectively the wet and dry seasons of Ningbo. Therefore, the
418 frequent rainfall events and larger upstream flow may reduce the significance of microplastic
419 point sources along Fenghua River urban section in winter, but increase the influence of non-
420 points source discharge (Xu et al., 2020b). To further explore these relationships, sampling over
421 multiple days in summer and winter to generate seasonal averages at each individual site was
422 likely necessary; however, sampling at both a high spatial and temporal resolution was not
423 plausible here and raises important questions about the resolution of data needed to make
424 meaningful estimates of microplastic concentrations and fluxes at sites (Stanton et al., 2020).

425

426 **4.2.2. Urban factors**

427 Urban factors are usually thought to shape microplastic distribution patterns. For example,
428 Wang et al. (2017) noticed microplastic concentrations declined with the distance from urban
429 centers. The concentration of microplastics in waterbodies was found to positively correlate to
430 the unit gross domestic product (GDP) or the unit population density where the sampling site
431 was located (Fan et al., 2019; Peng et al., 2018). In addition, studies have reported that
432 microplastic pollution in urban waterbodies is related to local land-use functions (Peng et al.,
433 2018). Despite microplastic concentrations being spatially heterogeneous in this study, there

434 were no obvious trends from the upstream (FH1) to downstream (FH43) in microplastic
435 concentration according to linear regression analysis (Tab. S2), supported by the NMDS results
436 (Fig. S1). Therefore, the distance from the sampling site to city center was not a determining
437 factor in microplastic pollution in the surface water in this study river.

438 Land-use types were grouped but, again, no significant differences in microplastic
439 concentrations were found according to Kruskal-Wallis tests (Tab. S4). This study defined land-
440 use types within 1 km of both banks of the Fenghua River; however, the actual use of the land
441 is difficult to quantify; land-use classification can include a range of potential microplastic
442 sources (e.g. a textile factory in comparison to a different industry); and land-use conditions
443 may integrate and overlap, such as industrial workshops on agricultural land and business
444 offices in residential buildings (Liu et al., 2008). Also, land use from further away may still
445 provide sources of microplastic to the Fenghua River, further complicating relationships
446 between land-use and microplastic concentrations.

447 No significant linear relationships were found between GDP density or population density and
448 microplastic concentrations (Tab. S2). We interpret the lack of strong relationship between
449 microplastic concentration and land-use and socio-economic variables as being due to the
450 inherent complexity and spatial heterogeneity of urban environments. We suspect that land-use
451 and socio-economic factors do influence microplastic concentrations but the over-lapping
452 nature of these variables and accumulation of microplastics downstream complicates the ability
453 to determine clear relationships. The semi-urban area tends to have a larger diversity of
454 microplastics compared to those found in the transitional and center-urban areas (Fig. S1). This

455 may be explained by the fact that the semi-urban area includes both primary and secondary
456 industries (e.g. agricultural and industrial production) while the city center is occupied more by
457 business and commercial services.

458 Although the 18 sluices along Fenghua River were suspected to be the point sources of
459 microplastic pollution in this study, the Mann-Whitney test results of sluice factors showed that
460 the presence or absence of sluices made no significant influences (Tab. S5). One explanation is
461 that the sampling in this study did not capture the opening time of sluices, which may lead to a
462 short duration increase in concentrations that are rapidly washed downstream. Another
463 explanation is that sluices do not represent a major factor of microplastic abundance patterns in
464 Fenghua River.

465

466 4.3. Insights and suggestions

467 Our research found that the influence of urban factors on microplastic pollution in fluvial
468 surface water was complex, with no statistical significance emerging. Statistically significant
469 patterns in microplastic distributions in urban environments from other studies tend to be where
470 the environmental matrix is relatively stable. For example, Wang et al. (2017) documented
471 microplastic concentrations decreased with the distance from the urban center in the surface
472 water of urban lakes linearly ($p < 0.001$). Moreover, Fan et al. (2019) reported the linear
473 relationship between microplastic concentration and population density as well as GDP ($p <$
474 0.01) in river sediment. In contrast, the high potential for diffusion and transportation of
475 microplastics in surface waters associated with waves, currents and other hydraulic and

476 anthropogenic factors, are likely to lead to the lack of obvious relationship between microplastic
477 concentrations and urban factors. This also demonstrates the complicating factor that fluvial
478 transport is likely to have when trying to attribute a source to microplastic pollution. It also has
479 implications for site selection when studying microplastics, especially where sampling
480 networks are less dense than that used here, with estimates of microplastic concentrations in
481 fluvial surface water potentially varying over several orders of magnitude depending on the
482 location selected (Stanton et al., 2020). The findings of this work further support the need for
483 comprehensive sampling campaigns when microplastic concentrations are being investigated,
484 and especially when microplastic fluxes are calculated.

485

486 5. Conclusion

487 In this study, the microplastic pollution of surface waters was quantified along the Fenghua
488 River, a major urban river of Ningbo City, Zhejiang Province. The results showed that
489 microplastic pollution was detected in all samples in summer and winter, and concentrations
490 varied widely from 300 n/m³ to 4000 n/m³ (0.3 – 4.0 n/L), with an average of 1620.16 ± 878.22
491 n/m³ (1.62 ± 0.88 n/L) in summer and 1696.08 ± 983.52 n/m³ (1.70 ± 0.98 n/L) in winter. Fibers
492 were the most common microplastic shape, while microplastics smaller than 1 mm were the
493 most numerous. Transparency was the most common color and PP was the most common
494 polymer type. Statistical trend is difficult to be observed from the spatial heterogeneity of
495 microplastic concentrations and typology along the river, which might be led by the
496 combination of the spatially dense sampling network and the complex transport of microplastics

497 through urban river environments. Future research work should focus on distinguishing
498 microplastics from point and non-point sources to determine the relative significance of
499 contributions, and the quantification of microplastic typologies.

500

501 **Acknowledgement**

502 This work was supported by funding from the Ningbo Social Development Project, Ningbo
503 Science and Technology Bureau, China (grant no. 2014C50011/201401C5008005), the
504 National Natural Science Foundation of China (NSFC) (grant no. 41850410497) and the
505 Faculty of Science and Engineering Postgraduate Research Grant 2018/21– University of
506 Nottingham Ningbo China; the National Key R&D Program of China (2019YFC1510400). The
507 authors would like to acknowledge their funders for enabling this research to take place.

508

509

510

511

512

513

514

515 **References**

- 516 Caruso, G., 2019. Microplastics as vectors of contaminants. *Mar. Pollut. Bull.* 146, 921–924.
517 <https://doi.org/10.1016/j.marpolbul.2019.07.052>
- 518 Crawford, C.B., Quinn, B., 2017. 9 - Microplastic separation techniques, in: Crawford, C.B., Quinn,
519 B.B.T.-M.P. (Eds.), . Elsevier, pp. 203–218. [https://doi.org/10.1016/B978-0-12-809406-](https://doi.org/10.1016/B978-0-12-809406-8.00009-8)
520 [8.00009-8](https://doi.org/10.1016/B978-0-12-809406-8.00009-8)
- 521 Deng, H., Wei, R., Luo, W., Hu, L., Li, B., Di, Y., Shi, H., 2020. Microplastic pollution in water and
522 sediment in a textile industrial area. *Environ. Pollut.* 258, 113658.
523 <https://doi.org/10.1016/j.envpol.2019.113658>
- 524 Di, M., Liu, X., Wang, W., Wang, J., 2019. Manuscript prepared for submission to environmental
525 toxicology and pharmacology pollution in drinking water source areas: Microplastics in the
526 Danjiangkou Reservoir, China. *Environ. Toxicol. Pharmacol.* 65, 82–89.
527 <https://doi.org/10.1016/j.etap.2018.12.009>
- 528 Ding, L., Mao, R. fan, Guo, X., Yang, X., Zhang, Q., Yang, C., 2019. Microplastics in surface waters
529 and sediments of the Wei River, in the northwest of China. *Sci. Total Environ.* 667, 427–
530 434. <https://doi.org/10.1016/j.scitotenv.2019.02.332>
- 531 Dong, M., Luo, Z., Jiang, Q., Xing, X., Zhang, Q., Sun, Y., 2020. The rapid increases in
532 microplastics in urban lake sediments. *Sci. Rep.* 10, 848. [https://doi.org/10.1038/s41598-](https://doi.org/10.1038/s41598-020-57933-8)
533 [020-57933-8](https://doi.org/10.1038/s41598-020-57933-8)
- 534 Eerkes-Medrano, D., Thompson, R.C., Aldridge, D.C., 2015. Microplastics in freshwater systems:
535 A review of the emerging threats, identification of knowledge gaps and prioritisation of
536 research needs. *Water Res.* 75, 63–82. <https://doi.org/10.1016/j.watres.2015.02.012>
- 537 Fan, Y., Zheng, K., Zhu, Z., Chen, G., Peng, X., 2019. Distribution, sedimentary record, and
538 persistence of microplastics in the Pearl River catchment, China. *Environ. Pollut.* 251, 862–
539 870. <https://doi.org/10.1016/j.envpol.2019.05.056>
- 540 Feng, S., Lu, H., Tian, P., Xue, Y., Lu, J., Tang, M., Feng, W., 2020. Analysis of microplastics in a
541 remote region of the Tibetan Plateau: Implications for natural environmental response to
542 human activities. *Sci. Total Environ.* 739, 140087.
543 <https://doi.org/10.1016/j.scitotenv.2020.140087>
- 544 Garside, M., 2019. Plastic materials production worldwide by region 2018 | Statista.
- 545 Geographical Information Monitoring Cloud Platform, 2020a. National GDP kilometer grid data
546 products.
- 547 Geographical Information Monitoring Cloud Platform, 2020b. National Population Density Data
548 Products.
- 549 Gong, P., Chen, B., Li, Xuecao, Liu, H., Wang, J., Bai, Y., Chen, J., Chen, X., Fang, L., Feng, S.,
550 Feng, Y., Gong, Y., Gu, H., Huang, H., Huang, X., Jiao, H., Kang, Y., Lei, G., Li, A., Li,
551 Xiaoting, Li, Xun, Li, Y., Li, Zhilin, Li, Zhongde, Liu, Chong, Liu, Chunxia, Liu, M., Liu,
552 S., Mao, W., Miao, C., Ni, H., Pan, Q., Qi, S., Ren, Z., Shan, Z., Shen, S., Shi, M., Song,
553 Y., Su, M., Ping Suen, H., Sun, B., Sun, F., Sun, J., Sun, L., Sun, W., Tian, T., Tong, X.,
554 Tseng, Y., Tu, Y., Wang, H., Wang, L., Wang, X., Wang, Z., Wu, T., Xie, Y., Yang, Jian,
555 Yang, Jun, Yuan, M., Yue, W., Zeng, H., Zhang, K., Zhang, N., Zhang, T., Zhang, Y., Zhao,
556 F., Zheng, Y., Zhou, Q., Clinton, N., Zhu, Z., Xu, B., 2020. Mapping essential urban land

557 use categories in China (EULUC-China): preliminary results for 2018. *Sci. Bull.* 65, 182–
558 187. <https://doi.org/10.1016/j.scib.2019.12.007>

559 GOSC, 2020. The reply of the State Council on the overall Urban Planning of Ningbo.

560 Guen, C.L., Suaria, G., Sherley, R.B., Ryan, P.G., Brierley, A.S., 2019. Microplastic study reveals
561 the presence of natural and synthetic fibres in the diet of King Penguins (*Aptenodytes*
562 *patagonicus*) foraging from South Georgia. *Environ. Int.* 134.
563 <https://doi.org/10.1016/j.envint.2019.105303>

564 Han, M., Niu, X., Tang, M., Zhang, B.-T., Wang, G., Yue, W., Kong, X., Zhu, J., 2020. Distribution
565 of microplastics in surface water of the lower Yellow River near estuary. *Sci. Total Environ.*
566 707, 135601. <https://doi.org/10.1016/j.scitotenv.2019.135601>

567 Horton, A.A., Walton, A., Spurgeon, D.J., Lahive, E., Svendsen, C., 2017. Microplastics in
568 freshwater and terrestrial environments: Evaluating the current understanding to identify
569 the knowledge gaps and future research priorities. *Sci. Total Environ.* 586, 127–141.
570 <https://doi.org/10.1016/j.scitotenv.2017.01.190>

571 Hu, L., Chernick, M., Hinton, D.E., Shi, H., 2018. Microplastics in Small Waterbodies and Tadpoles
572 from Yangtze River Delta, China. *Environ. Sci. Technol.* 52, 8885–8893.
573 <https://doi.org/10.1021/acs.est.8b02279>

574 Industry, C.P., 2019. More than 60 million plastic tablewares are consumed everyday in China (in
575 Chinese). *China Plast. Ind.* 47, 154.

576 Jiang, C., Yin, L., Li, Z., Wen, X., Luo, X., Hu, S., Yang, H., Long, Y., Deng, B., Huang, L., Liu, Y.,
577 2019. Microplastic pollution in the rivers of the Tibet Plateau. *Environ. Pollut.* 249, 91–98.
578 <https://doi.org/10.1016/j.envpol.2019.03.022>

579 Lam, T.W.L., Fok, L., Lin, L., Xie, Q., Li, H.-X., Xu, X.-R., Yeung, L.C., 2020. Spatial variation of
580 floatable plastic debris and microplastics in the Pearl River Estuary, South China. *Mar.*
581 *Pollut. Bull.* 158, 111383. <https://doi.org/10.1016/j.marpolbul.2020.111383>

582 Lehtiniemi, M., Hartikainen, S., Näkki, P., Engström-Öst, J., Koistinen, A., Setälä, O., 2018. Size
583 matters more than shape: Ingestion of primary and secondary microplastics by small
584 predators. *Food Webs* 17, e00097. <https://doi.org/10.1016/j.fooweb.2018.e00097>

585 Li, F., Yang, L., 2016. A Research on the Development of Ningbo's Cross-border E-commerce. *Spec.*
586 *Zone Econ.* 47–49.

587 Li, X., Ji, Y., Mei, Q., Chen, L., Zhang, X., Dong, B., Dai, X., 2019. Review of Microplastics in
588 Wastewater and Sludge of Wastewater Treatment Plant. *Water Purif. Technol.* 38, 13–22,84.
589 <https://doi.org/10.15890/j.cnki.jsjs.2019.07.003>

590 Li, Y., Lu, Z., Zheng, H., Wang, J., Chen, C., 2020. Microplastics in surface water and sediments of
591 Chongming Island in the Yangtze Estuary, China. *Environ. Sci. Eur.* 32, 15.
592 <https://doi.org/10.1186/s12302-020-0297-7>

593 Lin, L., Zuo, L.-Z., Peng, J.-P., Cai, L.-Q., Fok, L., Yan, Y., Li, H.-X., Xu, X.-R., 2018. Occurrence
594 and distribution of microplastics in an urban river: A case study in the Pearl River along
595 Guangzhou City, China. *Sci. Total Environ.* 644, 375–381.
596 <https://doi.org/10.1016/j.scitotenv.2018.06.327>

597 Liu, K., Wang, X., Song, Z., Wei, N., Ye, H., Cong, X., Zhao, L., Li, Y., Qu, L., Zhu, L., Zhang, F.,
598 Zong, C., Jiang, C., Li, D., 2020. Global inventory of atmospheric fibrous microplastics
599 input into the ocean: An implication from the indoor origin. *J. Hazard. Mater.* 400, 123223.
600 <https://doi.org/10.1016/j.jhazmat.2020.123223>

601 Liu, S., Jian, M., Zhou, L., Li, W., Wu, X., Rao, D., 2019. Pollution Characteristics of Microplastics
602 in Migratory Bird Habitats Located Within Poyang Lake Wetlands. *Environ. Sci.* 40, 2639–
603 2646. <https://doi.org/10.13227/j.hjx.201812111>

604 Liu, W., Zhang, D., Chen, B., 2008. Characteristics of China's Town-level Land Use in Rapid
605 Urbanization Stage. *ACTA Geogr. Sin.* 301–310.

606 Lloyd's List, 2019. One Hundred Ports.

607 Ma, J., Niu, X., Zhang, D., Lu, L., Ye, X., Deng, W., Li, Y., Lin, Z., 2020. High levels of microplastic
608 pollution in aquaculture water of fish ponds in the Pearl River Estuary of Guangzhou, China.
609 *Sci. Total Environ.* 744, 140679. <https://doi.org/10.1016/j.scitotenv.2020.140679>

610 National Bureau of Statistics of China, 2020. China Statistical Yearbook.

611 NDRC, 2020. Circular of the National Development and Reform Commission on the Issuance of
612 Regional Planning for the Yangtze River Delta Region.

613 NDRC, 2007. Test method for identification of textile fibers - Part 3: Microscopy (FZ/T 01057.3-
614 2007).

615 Pan, Z., Sun, Y., Liu, Q., Lin, C., Sun, X., He, Q., Zhou, K., Lin, H., 2020. Riverine microplastic
616 pollution matters: A case study in the Zhangjiang River of Southeastern China. *Mar. Pollut.*
617 *Bull.* 159, 111516. <https://doi.org/10.1016/j.marpolbul.2020.111516>

618 Peng, G., Xu, P., Zhu, B., Bai, M., Li, D., 2018. Microplastics in freshwater river sediments in
619 Shanghai, China: A case study of risk assessment in mega-cities. *Environ. Pollut.* 234, 448–
620 456. <https://doi.org/10.1016/j.envpol.2017.11.034>

621 Rochman, C.M., Brookson, C., Bikker, J., Djuric, N., Earn, A., Bucci, K., Athey, S., Huntington, A.,
622 McIlwraith, H., Munno, K., De Frond, H., Kolomijeca, A., Erdle, L., Grbic, J., Bayoumi,
623 M., Borrelle, S.B., Wu, T., Santoro, S., Werbowski, L.M., Zhu, X., Giles, R.K., Hamilton,
624 B.M., Thaysen, C., Kaura, A., Klasios, N., Ead, L., Kim, J., Sherlock, C., Ho, A., Hung, C.,
625 2019. Rethinking microplastics as a diverse contaminant suite. *Environ. Toxicol. Chem.* 38,
626 703–711. <https://doi.org/10.1002/etc.4371>

627 Scheurer, M., Bigalke, M., 2018. Microplastics in Swiss Floodplain Soils. *Environ. Sci. Technol.*
628 52, 3591–3598. <https://doi.org/10.1021/acs.est.7b06003>

629 Stanton, T., Johnson, M., Nathanail, P., MacNaughtan, W., Gomes, R.L., 2020. Freshwater
630 microplastic concentrations vary through both space and time. *Environ. Pollut.* 263, 114481.
631 <https://doi.org/10.1016/j.envpol.2020.114481>

632 Stanton, T., Johnson, M., Nathanail, P., MacNaughtan, W., Gomes, R.L., 2019. Freshwater and
633 airborne textile fibre populations are dominated by 'natural', not microplastic, fibres. *Sci.*
634 *Total Environ.* 666, 377–389. <https://doi.org/10.1016/j.scitotenv.2019.02.278>

635 Su, L., Xue, Y., Li, L., Yang, D., Kolandhasamy, P., Li, D., Shi, H., 2016. Microplastics in Taihu
636 Lake, China. *Environ. Pollut.* 216, 711–719. <https://doi.org/10.1016/j.envpol.2016.06.036>

637 Suaria, G., Achtypi, A., Perold, V., Lee, J.R., Ryan, P.G., 2020. Microfibers in oceanic surface waters:
638 A global characterization. *Sci. Adv.* 6, eaay8493. <https://doi.org/10.1126/sciadv.aay8493>

639 Tang, Y., Chan, F.K.S., Griffiths, J., 2015. City Profile: Ningbo. *Cities* 42, 97–108.

640 Tien, C.-J., Wang, Z.-X., Chen, C.S., 2020. Microplastics in water, sediment and fish from the
641 Fengshan River system: Relationship to aquatic factors and accumulation of polycyclic
642 aromatic hydrocarbons by fish. *Environ. Pollut.* 265, 114962.
643 <https://doi.org/10.1016/j.envpol.2020.114962>

644 van Wijnen, J., Ragas, A.M.J., Kroeze, C., 2019. Modelling global river export of microplastics to

645 the marine environment: Sources and future trends. *Sci. Total Environ.* 673, 392–401.
646 <https://doi.org/10.1016/j.scitotenv.2019.04.078>

647 Wang, W., Ndungu, A.W., Li, Z., Wang, J., 2017. Microplastics pollution in inland freshwaters of
648 China: A case study in urban surface waters of Wuhan, China. *Sci. Total Environ.* 575,
649 1369–1374. <https://doi.org/10.1016/j.scitotenv.2016.09.213>

650 Wang, W., Yuan, W., Chen, Y., Wang, J., 2018. Microplastics in surface waters of Dongting Lake
651 and Hong Lake, China. *Sci. Total Environ.* 633, 539–545.
652 <https://doi.org/10.1016/j.scitotenv.2018.03.211>

653 Xu, X., Jian, Y., Xue, Y., Hou, Q., Wang, L., 2019. Microplastics in the wastewater treatment plants
654 (WWTPs): Occurrence and removal. *Chemosphere* 235, 1089–1096.
655 <https://doi.org/10.1016/j.chemosphere.2019.06.197>

656 Xu, Y., Chan, F.K.S., Johnson, M., Stanton, T., He, J., Jia, T., Wang, J., Wang, Z., Yao, Y., Yang, J.,
657 XU, Y., Yu, X., Liu, D., 2020a. Investigation of the Urban Factors Affecting Microplastic
658 Pollution in Chinese Cities: The Case of Ningbo. *Proc. 2020 Int. Conferece Resour. Sustain.*
659 *Sustain. Urban. BRI Era IcRS Urban.* 2020 325–341. [https://doi.org/doi.org/10.1007/978-](https://doi.org/doi.org/10.1007/978-981-15-9605-6_23)
660 [981-15-9605-6_23](https://doi.org/doi.org/10.1007/978-981-15-9605-6_23)

661 Xu, Yuyao, Chan, F.K.S., He, J., Johnson, M., Gibbins, C., Kay, P., Stanton, T., Xu, Yaoyang, Li, G.,
662 Feng, M., Paramor, O., Yu, X., Zhu, Y.-G., 2020b. A critical review of microplastic
663 pollution in urban freshwater environments and legislative progress in China:
664 Recommendations and insights. *Crit. Rev. Environ. Sci. Technol.* 1–44.
665 <https://doi.org/10.1080/10643389.2020.1801308>

666 Xue, B., Zhang, L., Li, R., Wang, Y., Guo, J., Yu, K., Wang, S., 2020. Underestimated Microplastic
667 Pollution Derived from Fishery Activities and “Hidden” in Deep Sediment. *Environ. Sci.*
668 *Technol.* 54, 2210–2217. <https://doi.org/10.1021/acs.est.9b04850>

669 Yan, M., Nie, H., Xu, K., He, Y., Hu, Y., Huang, Y., Wang, J., 2019. Microplastic abundance,
670 distribution and composition in the Pearl River along Guangzhou city and Pearl River
671 estuary, China. *Chemosphere* 217, 879–886.
672 <https://doi.org/10.1016/j.chemosphere.2018.11.093>

673 Ye, Q., 2020. Characteristics of micro-plastic pollution in Nanjing urban watars. *Energy Environ.*
674 *Prot.* 34, 79–83.

675 Yuan, W., Liu, X., Wang, W., Di, M., Wang, J., 2019. Microplastic abundance, distribution and
676 composition in water, sediments, and wild fish from Poyang Lake, China. *Ecotoxicol.*
677 *Environ. Saf.* 170, 180–187. <https://doi.org/10.1016/j.ecoenv.2018.11.126>

678 Zhang, K., Shi, H., Peng, J., Wang, Y., Xiong, X., Wu, C., Lam, P.K.S., 2018. Microplastic pollution
679 in China’s inland water systems: A review of findings, methods, characteristics, effects, and
680 management. *Sci. Total Environ.* 630, 1641–1653.
681 <https://doi.org/10.1016/j.scitotenv.2018.02.300>

682 Zhang, Y., Kang, S., Allen, S., Allen, D., Gao, T., Sillanpää, M., 2020. Atmospheric microplastics:
683 A review on current status and perspectives. *Earth-Sci. Rev.* 203, 103118.
684 <https://doi.org/10.1016/j.earscirev.2020.103118>

685 Zhao, S., Zhu, L., Wang, T., Li, D., 2014. Suspended microplastics in the surface water of the
686 Yangtze Estuary System, China: First observations on occurrence, distribution. *Mar. Pollut.*
687 *Bull.* 86, 562–568. <https://doi.org/10.1016/j.marpolbul.2014.06.032>

688 Zhao, W., Huang, W., Yin, M., Huang, P., Ding, Y., Ni, X., Xia, H., Liu, H., Wang, G., Zheng, H.,

689 Cai, M., 2020. Tributary inflows enhance the microplastic load in the estuary: A case from
690 the Qiantang River. *Mar. Pollut. Bull.* 156, 111152.
691 <https://doi.org/10.1016/j.marpolbul.2020.111152>

692 Zhou, G., Wang, Q., Zhang, J., Li, Q., Wang, Y., Wang, M., Huang, X., 2020. Distribution and
693 characteristics of microplastics in urban waters of seven cities in the Tuojiang River basin,
694 China. *Environ. Res.* 189, 109893. <https://doi.org/10.1016/j.envres.2020.109893>

695 Zou, Y., Xu, Q., Zhang, G., Wang, Y., Liu, C., Zheng, H., Li, F., 2017. Review on the joint toxicity
696 of microplastics and pesticide pollution. *Asian J. Ecotoxicol.* 12, 25–33.
697 <https://doi.org/10.7524/AJE.1673-5897.20170518001>

698

699

700 **Appendix: Supplementary document**701 **Table S1. Location and land-use condition of all sampling sites**

Site	Closest land-use condition	Location	Distance to city center (km)
FH1	Construction area	N 29°46'11.88"/E 121°26'52.20"	15.8
FH2	Farmland	N 29°46'37.97"/E 121°27'02.85"	15.1
FH3	Village	N 29°46'43.14"/E 121°26'39.40"	15.4
FH4	Industrial area	N 29°47'01.66"/E 121°26'29.89"	15.2
FH5	Administration area	N 29°47'14.28"/E 121°26'43.70"	14.7
FH6	Village	N 29°47'00.68"/E 121°27'11.20"	14.4
FH7	Unused area	N 29°46'40.86"/E 121°27'23.00"	14.6
FH8	Farmland	N 29°47'00.22"/E 121°27'28.62"	14.1
FH9	Village	N 29°47'10.40"/E 121°27'36.68"	13.7
FH10	Farmland	N 29°47'11.38"/E 121°27'44.29"	13.5
FH11	Farmland	N 29°47'12.68"/E 121°27'35.89"	13.6
FH12	Administration area	N 29°47'24.06"/E 121°28'08.53"	12.6
FH13	Farmland	N 29°47'19.75"/E 121°28'20.71"	12.6
FH14	Administration area	N 29°47'32.98"/E 121°28'36.14"	12.1
FH15	Village	N 29°47'38.09"/E 121°28'37.74"	12.0
FH16	Residential area	N 29°47'20.19"/E 121°28'02.64"	11.9
FH17	Farmland	N 29°47'28.49"/E 121°29'22.26"	11.3
FH18	Farmland	N 29°47'50.82"/E 121°29'17.06"	10.9
FH19	Industrial area	N 29°47'40.89"/E 121°30'01.56"	10.6
FH20	Farmland	N 29°47'39.93"/E 121°29'49.49"	10.5
FH21	Greenspace	N 29°47'28.32"/E 121°30'28.29"	10.4
FH22	Farmland	N 29°47'31.56"/E 121°30'22.02"	10.4
FH23	Greenspace	N 29°48'06.48"/E 121°30'10.62"	9.6
FH24	Greenspace	N 29°48'24.14"/E 121°30'23.25"	9.0
FH25	Greenspace	N 29°48'18.32"/E 121°30'51.70"	8.7
FH26	Greenspace	N 29°48'25.77"/E 121°30'56.06"	8.5
FH27	Greenspace	N 29°48'43.42"/E 121°30'54.49"	8.1
FH28	Greenspace	N 29°48'57.44"/E 121°31'15.51"	7.3
FH29	Greenspace	N 29°49'19.11"/E 121°30'44.69"	7.3
FH30	Greenspace	N 29°49'21.00"/E 121°30'46.65"	7.3
FH31	Greenspace	N 29°49'36.33"/E 121°30'29.58"	7.1
FH32	Administration area	N 29°49'46.96"/E 121°31'46.96"	6.0
FH33	Greenspace	N 29°49'59.32"/E 121°31'24.98"	5.7
FH34	Greenspace	N 29°50'25.11"/E 121°31'23.58"	5.0
FH35	Greenspace	N 29°50'32.88"/E 121°31'48.76"	4.4
FH36	Residential area	N 29°51'11.32"/E 121°31'50.82"	3.5
FH37	Residential area	N 29°51'15.01"/E 121°31'5.22"	3.2
FH38	Residential area	N 29°51'14.67"/E 121°32'27.46"	2.8
FH39	Residential area	N 29°51'23.88"/E 121°32'47.79"	2.3

FH40	Greenspace	N 29°51'35.43"/E 121°32'57.57"	1.9
FH41	Greenspace	N 29°51'48.64"/E 121°33'11.35"	1.4
FH42	Greenspace	N 29°52'7.97"/E 121°33'17.89"	0.7
FH43	Greenspace	N 29°52'28.41"/E 121°33'20.36"	0.1

702

703

704 Table S2 Linear regression analysis results (R^2 value) of the relationships between microplastic
705 concentrations and (a) straight-line distance from sampling sites to city center, (b) the order of sampling
706 sites, (c) population density and (d) GDP density

R^2 value of linear regression for 43 summer samples	Distance from city center	Order of sampling points	Population density	GDP density
Total concentration	0.054	0.063	0.002	0.000
Fragment concentration	0.011	0.017	0.001	0.002
Fiber concentration	0.055	0.087	0.003	0.001
Film concentration	0.011	0.022	0.000	0.000
Pellet/foam concentration	0.058	0.061	0.019	0.15
Microplastics in size of 0-0.5mm	0.040	0.059	0.001	0.000
Microplastics in size of 0.5-1mm	0.009	0.210	0.213	0.231
Microplastics in size of 1-2mm	0.009	0.026	0.009	0.014
Microplastics in size of 2-3mm	0.162	0.197	0.120	0.111
Microplastics in size of 3-4mm	0.020	0.017	0.009	0.007
Microplastics in size of 4-5mm	0.031	0.032	0.022	0.020
Microplastics in yellow	0.080	0.081	0.051	0.045
Microplastics in transparent	0.025	0.050	0.001	0.002
Microplastics in red	0.036	0.053	0.002	0.001
Microplastics in brown	0.022	0.015	0.048	0.050
Microplastics in blue	0.090	0.110	0.025	0.021
Microplastics in black	0.003	0.007	0.000	0.000
Microplastics in green	0.054	0.070	0.018	0.015
Microplastics in white	0.000	0.000	0.011	0.012
Microplastics in purple	0.011	0.013	0.035	0.036
Microplastics in grey	0.000	0.000	0.014	0.015
Microplastics in other colors	0.029	0.026	0.039	0.037

707

708 Table S3 Kruskal-Wallis test results for investigating the microplastic concentration variations among
709 semi-urban group, transition group and city center group of sampling sites

Kruskal-Wallis for 43 summer samples in three different GDP/population groups	<i>p</i> value
Total concentration	0.171
Fragment concentration	0.356
Fiber concentration	0.306
Film concentration	0.905
Pellet/foam concentration	0.238
Concentrations of microplastics in 0-0.5mm	0.305
Concentrations of microplastics in 0.5-1mm	0.148

Concentrations of microplastics in 1-2mm	0.154
Concentrations of microplastics in 2-3mm	0.036
Concentrations of microplastics in 3-4mm	0.424
Concentrations of microplastics in 4-5mm	0.683
Concentrations of microplastics in yellow	0.387
Concentrations of microplastics in transparent	0.373
Concentrations of microplastics in red	0.802
Concentrations of microplastics in brown	0.546
Concentrations of microplastics in blue	0.143
Concentrations of microplastics in black	0.550
Concentrations of microplastics in green	0.296
Concentrations of microplastics in white	0.529
Concentrations of microplastics in purple	0.546
Concentrations of microplastics in grey	0.315
Concentrations of microplastics in other colors	0.477

710

711

712

Table S4 Kruskal-Wallis analysis results for investigating land-use factors on microplastic concentrations

Kruskal-Wallis test for land-use factors on 43 summer samples	<i>p</i> value
Total concentration	0.717
Fragment concentration	0.551
Fiber concentration	0.741
Film concentration	0.229
Pellet/foam concentration	0.593
Concentrations of microplastics in 0-0.5mm	0.732
Concentrations of microplastics in 0.5-1mm	0.883
Concentrations of microplastics in 1-2mm	0.327
Concentrations of microplastics in 2-3mm	0.331
Concentrations of microplastics in 3-4mm	0.692
Concentrations of microplastics in 4-5mm	0.440
Concentrations of microplastics in yellow	0.082
Concentrations of microplastics in transparent	0.307
Concentrations of microplastics in red	0.967
Concentrations of microplastics in brown	0.349
Concentrations of microplastics in blue	0.596
Concentrations of microplastics in black	0.852
Concentrations of microplastics in green	0.881
Concentrations of microplastics in white	0.400
Concentrations of microplastics in purple	0.834
Concentrations of microplastics in grey	0.271
Concentrations of microplastics in other colors	0.723

713

714

715 Table S5 Mann-Whitney test for investigating the influences of water sluice on local microplastic
 716 concentration

Mann-Whitney test for sluice factor on 43 summer samples	<i>p</i> value
Total concentration	0.325
Fragment concentration	0.283
Fiber concentration	0.631
Film concentration	0.048
Pellet/foam concentration	0.688
Concentrations of microplastics in 0-0.5mm	0.115
Concentrations of microplastics in 0.5-1mm	0.444
Concentrations of microplastics in 1-2mm	0.892
Concentrations of microplastics in 2-3mm	0.803
Concentrations of microplastics in 3-4mm	0.473
Concentrations of microplastics in 4-5mm	0.058
Concentrations of microplastics in yellow	0.611
Concentrations of microplastics in transparent	0.204
Concentrations of microplastics in red	0.406
Concentrations of microplastics in brown	0.225
Concentrations of microplastics in blue	0.961
Concentrations of microplastics in black	0.193
Concentrations of microplastics in green	0.238
Concentrations of microplastics in white	0.901
Concentrations of microplastics in purple	0.840
Concentrations of microplastics in grey	0.696
Concentrations of microplastics in other colors	0.163

717
 718 Table S6 The Wilcoxon signed ranks test (paired samples non-parametric test) results of the seasonal
 719 differences between 17 summer samples and 17 winter samples

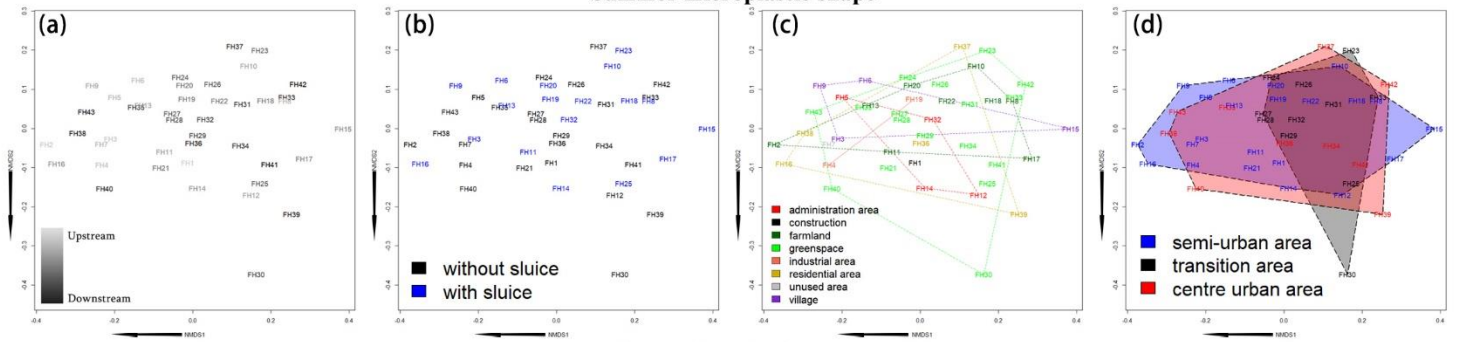
Wilcoxon test for summer and winter samples from 17 sampling sites	<i>p</i> value
Total summer and winter microplastic concentrations	0.723
Summer and winter fragment concentrations	0.434
Summer and winter fiber concentrations	0.925
Summer and winter film concentrations	0.103
Summer and winter pellet/foam concentrations	0.878
Summer and winter concentrations of microplastics in 0-0.5mm	0.868
Summer and winter concentrations of microplastics in 0.5-1mm	0.704
Summer and winter concentrations of microplastics in 1-2mm	0.538
Summer and winter concentrations of microplastics in 2-3mm	0.887
Summer and winter concentrations of microplastics in 3-4mm	0.813
Summer and winter concentrations of microplastics in 4-5mm	0.915
Summer and winter concentrations of microplastics in yellow	0.528
Summer and winter concentrations of microplastics in transparent	0.227
Summer and winter concentrations of microplastics in red	0.280
Summer and winter concentrations of microplastics in brown	0.785

Summer and winter concentrations of microplastics in blue	0.906
Summer and winter concentrations of microplastics in black	0.538
Summer and winter concentrations of microplastics in green	0.065
Summer and winter concentrations of microplastics in white	0.691
Summer and winter concentrations of microplastics in purple	0.317
Summer and winter concentrations of microplastics in grey	0.655
Summer and winter concentrations of microplastics in other colors	0.180

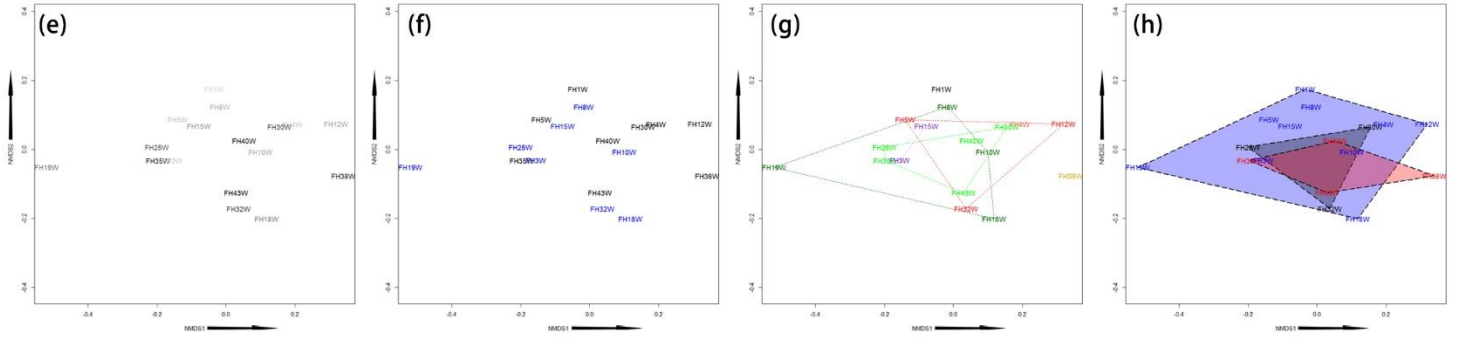
720

721

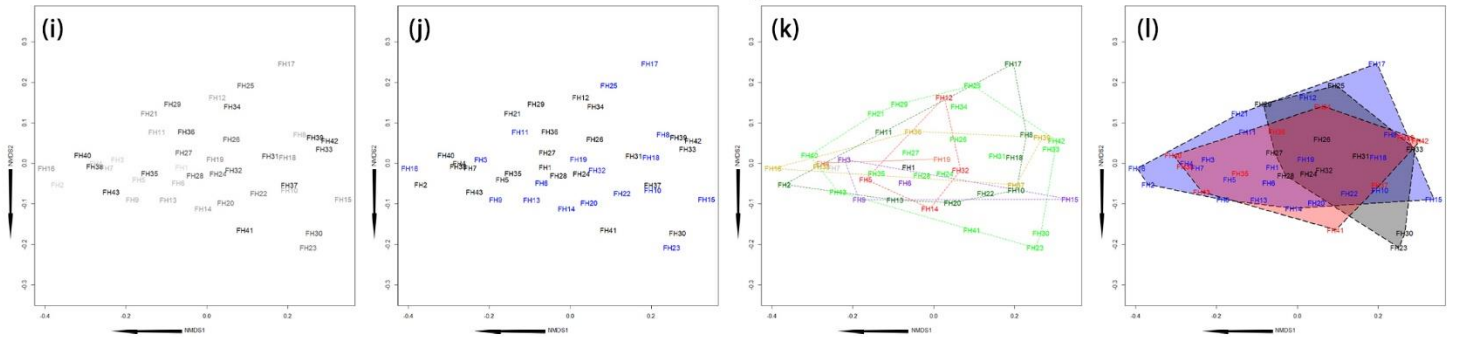
Summer microplastic shape



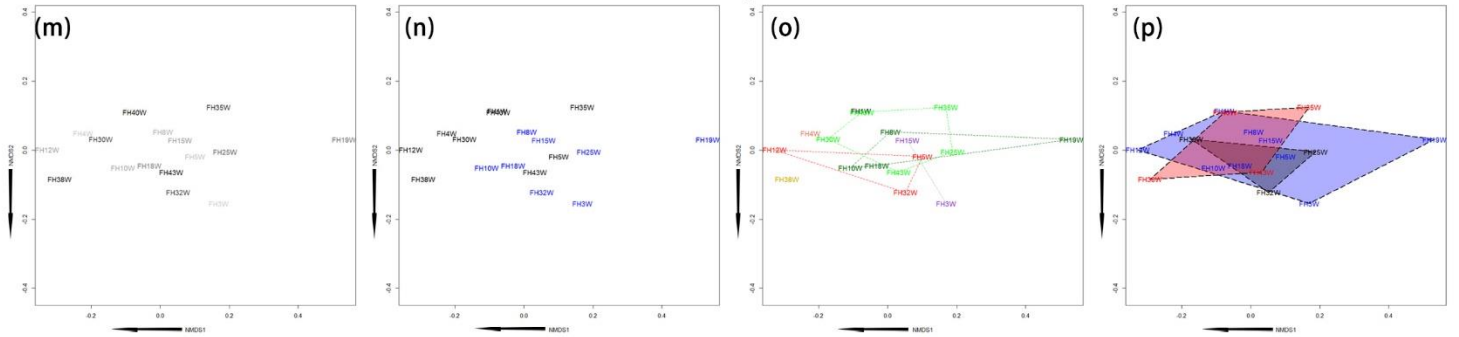
Winter microplastic shape



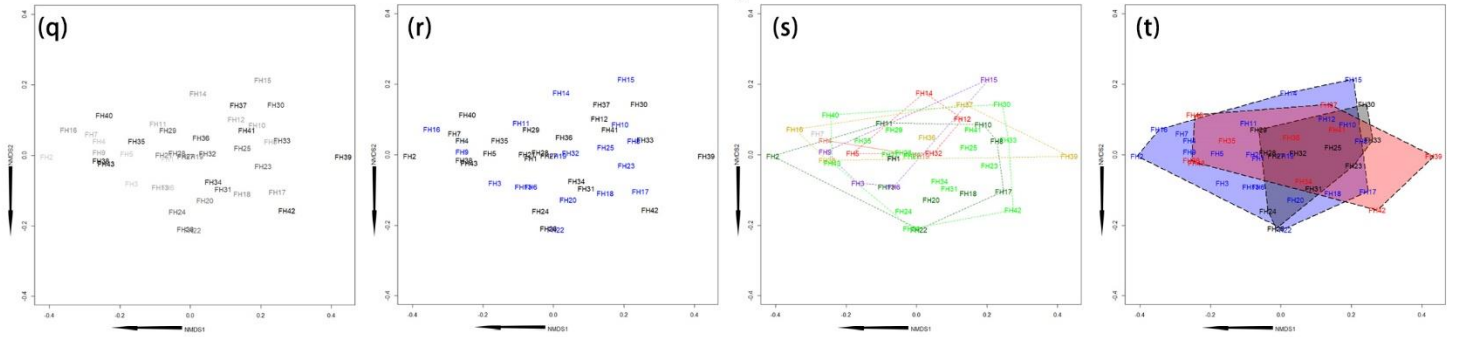
Summer microplastic size



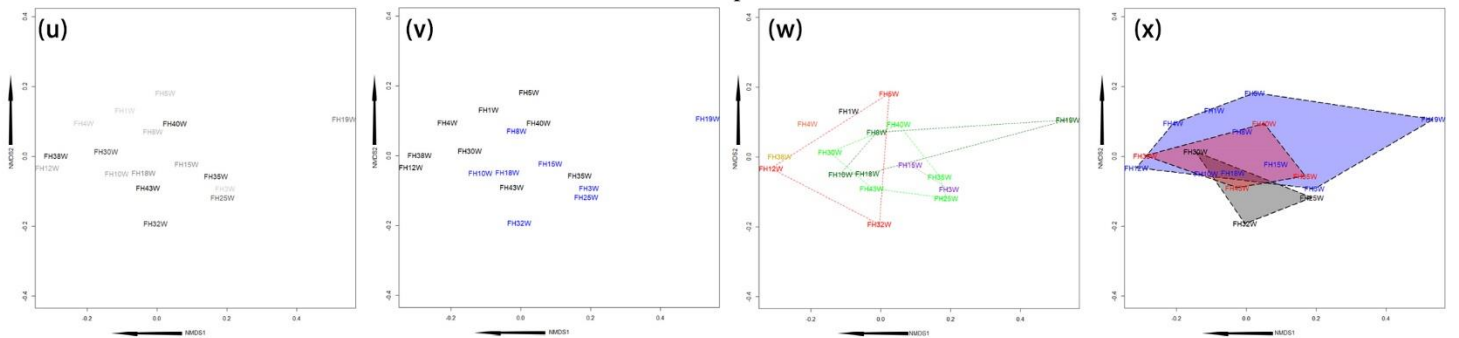
Winter microplastic size



Summer microplastic colour



Winter microplastic colour



723 Figure S1 (Previous page continued) n-MDS coordinate images. The horizontal axis of each graph is the
724 first non-metric dimension scale (NMDS1), and the vertical axis is the second non-metric dimension
725 scale (NMDS2). Taking Bray-Curtis dissimilarities as the proximity calculation standard, 43 summer
726 sampling points were scaled in coordinates (a-d), coordinates (i-l) and coordinates (q-t) by regarding
727 microplastics in different shapes (*Stress* = 0.121), size ranges (*Stress* = 0.087) and colors (*Stress* = 0.140)
728 as different microplastic ‘species’. In the same way, 17 winter sampling sites were scaled in coordinates
729 (e-h), coordinates (m-p) and coordinates (u-x) by regarding microplastics in different shapes (*Stress* =
730 0.053), size ranges (*Stress* = 0.039) and colors (*Stress* = 0.082) as different microplastic species. In
731 coordinates (a, e, i, m, q & u), the color of sampling site changes from light to dark from upstream to
732 downstream. In coordinates (b, f, j, n, r & v), the sampling sites in blue are affected by sluice factor while
733 the points in black are not. In coordinates (c, g, k, o, s & w), different colors were used to distinguish the
734 land-use types and dotted polygons to envelop the sampling sites in the same land-use types. In
735 coordinates (d, h, l, p, t & x), hull polygons in different colors were used to cover the sampling sites in
736 three urbanization levels.

737

738

739

740

741

742